

## Supplementary Information

# Wide Electrochemical Window Ionic Salt for use in Electropositive Metal Electrodeposition and Solid State Li-ion Batteries

*Sankaran Murugesan<sup>a</sup>, Oliver A. Quintero<sup>a</sup>, Brendan P. Chou<sup>a</sup>, Penghao Xiao<sup>a</sup>, Kyusung Park<sup>b</sup>, Justin W. Hall<sup>a</sup>, Richard A. Jones<sup>a</sup>, Graeme Henkelman<sup>a</sup>, John B. Goodenough<sup>b</sup> and Keith J. Stevenson<sup>a\*</sup>*

<sup>a</sup>Department of Chemistry and Biochemistry, The University of Texas at Austin, 1 University Station, Austin, Texas, 78712, USA

<sup>b</sup>Texas Materials Institute and Materials Science and Engineering Program, The University of Texas at Austin, Austin, Texas 78712, United States

---

\* Corresponding author: Keith J. Stevenson (stevenson@mail.cm.utexas.edu) (T) +1-512- 232-9160; (F) +1-512-471-8696

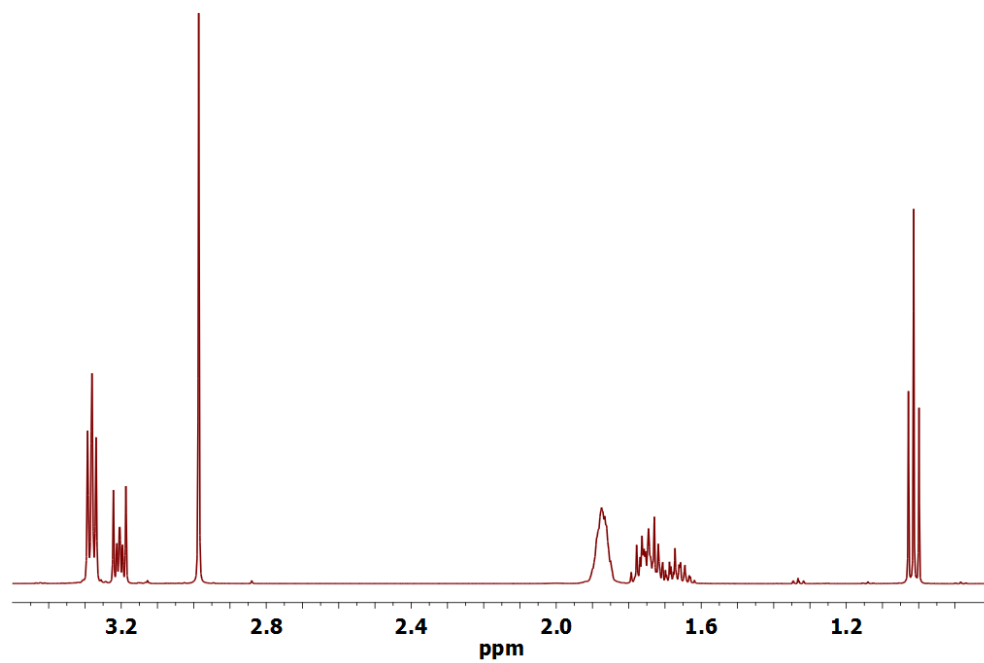


**Figure S1a.** <sup>1</sup>H NMR spectrum of PP<sub>13</sub>PF<sub>6</sub> in CD<sub>2</sub>Cl<sub>2</sub>.

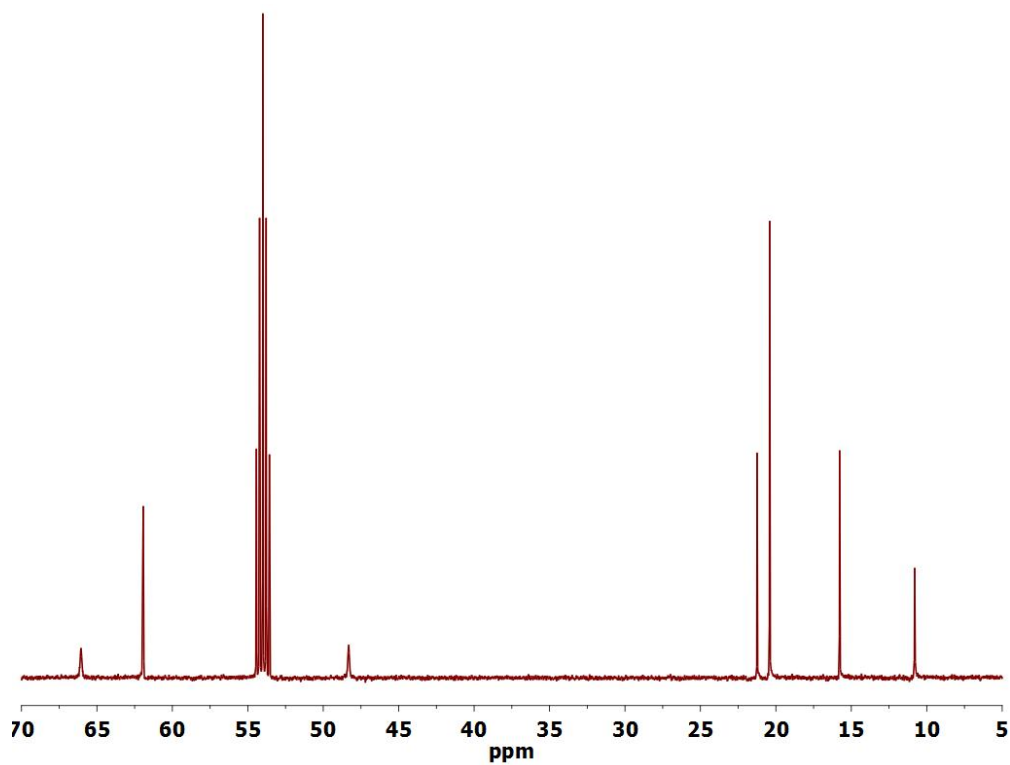


**Figure S1b.** <sup>13</sup>C NMR spectrum of PP<sub>13</sub>PF<sub>6</sub> in CD<sub>2</sub>Cl<sub>2</sub>.

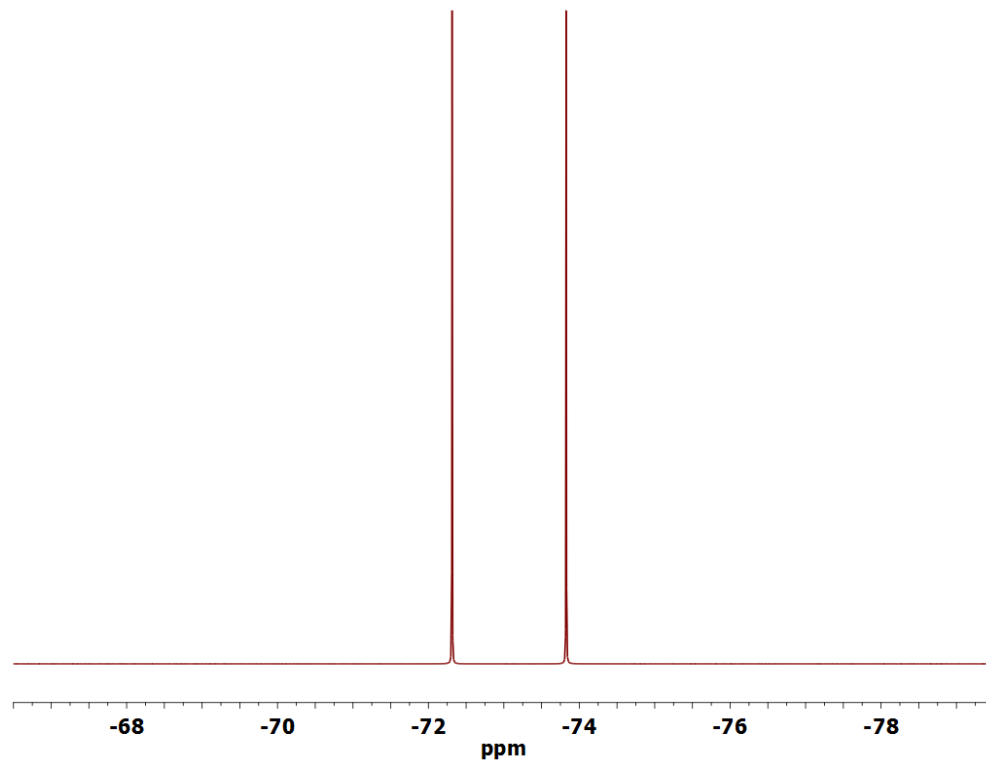


**Figure S1c.**  $^{19}\text{F}$  NMR spectrum of  $\text{PP}_{13}\text{PF}_6$  in  $\text{CD}_2\text{Cl}_2$ .

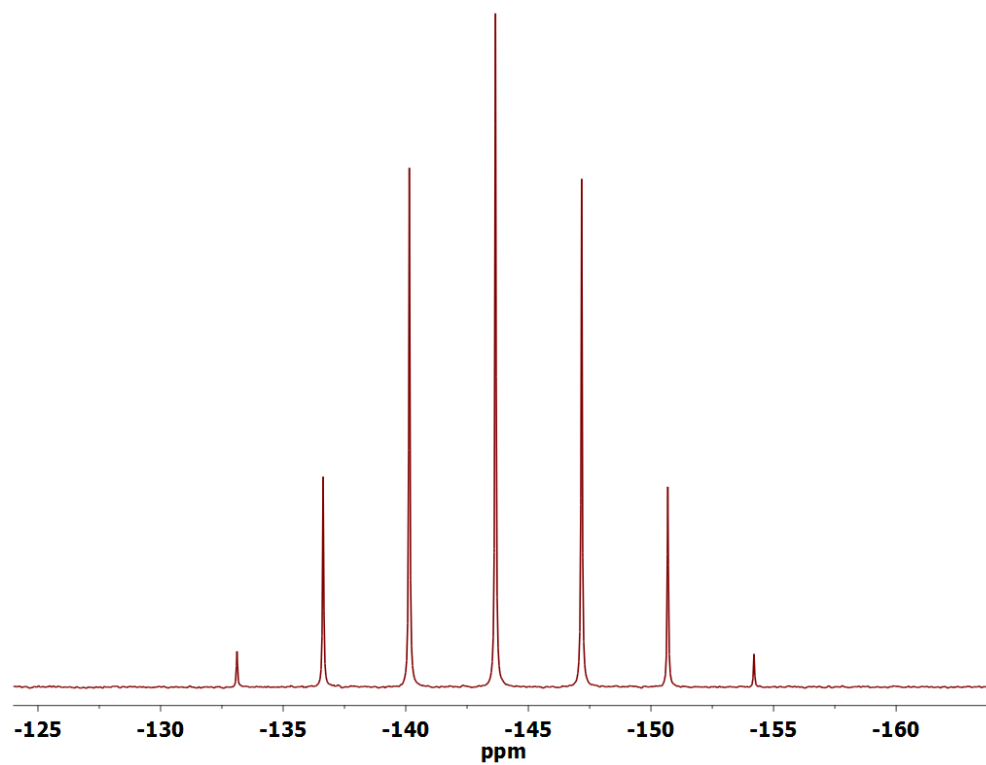


**Figure S1d.**  $^{31}\text{P}$  NMR spectrum of  $\text{PP}_{13}\text{PF}_6$  in  $\text{CD}_2\text{Cl}_2$ .

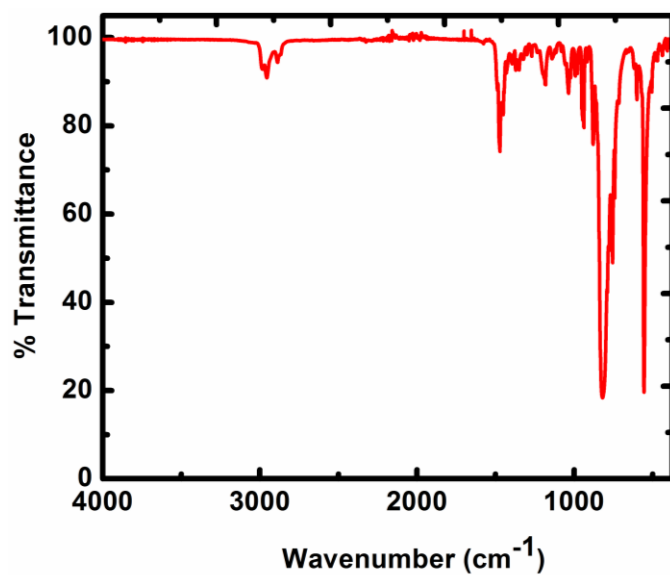


**Figure S1e.** FTIR (diamond ATR) spectrum of PP<sub>13</sub>PF<sub>6</sub>.

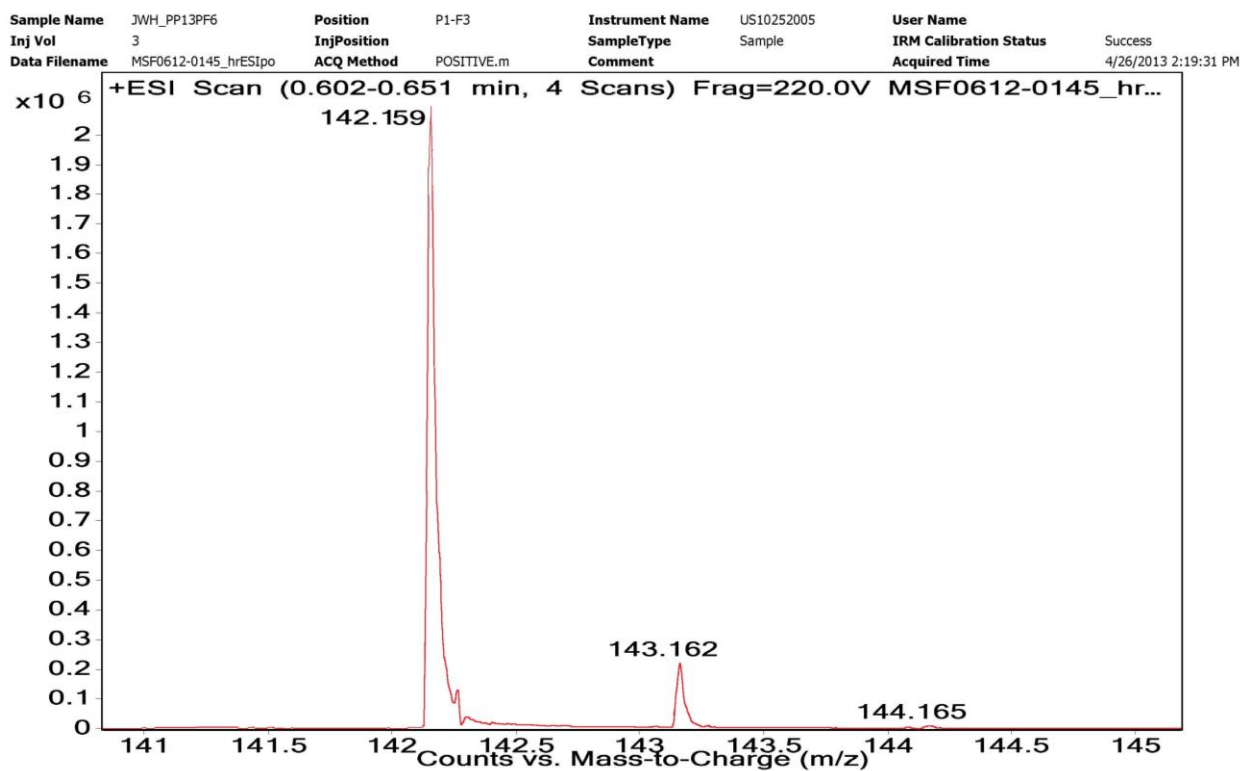


**Figure S1f.** Positive ion mass spectrum of PP<sub>13</sub>PF<sub>6</sub>.

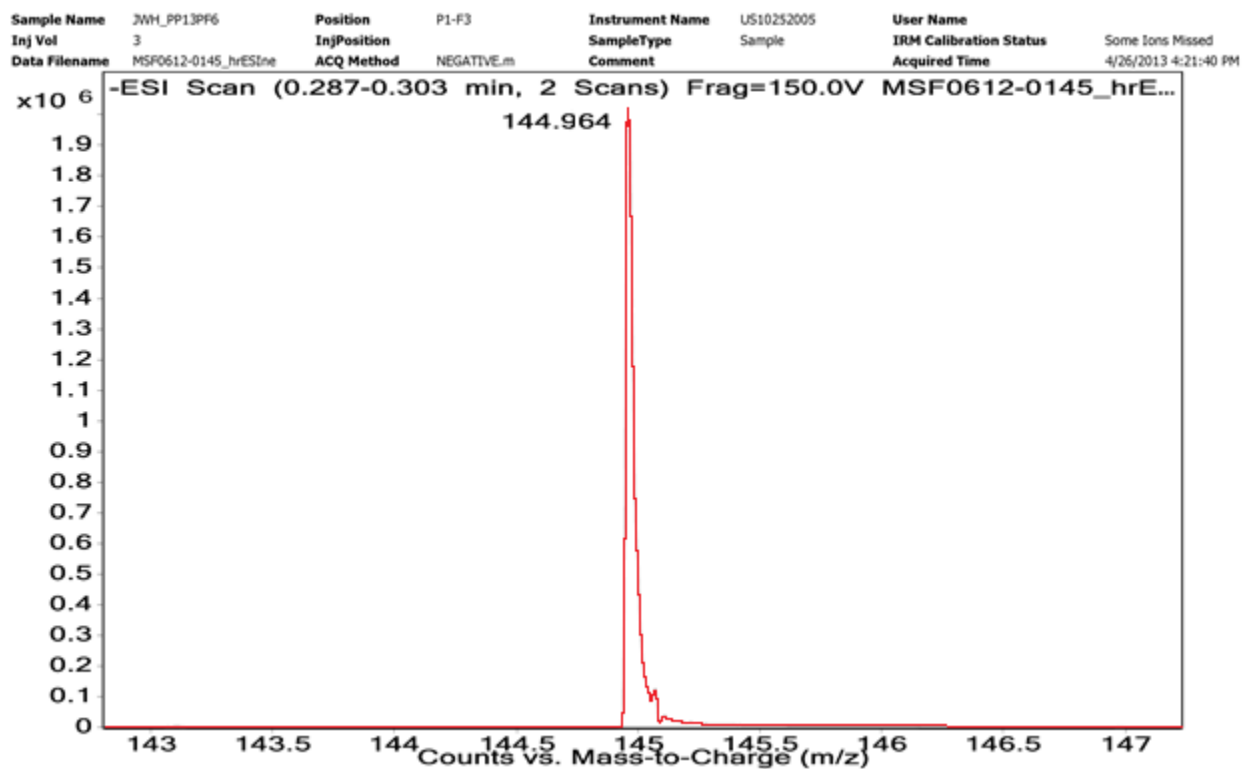


**Figure S1g.** Negative ion mass spectrum of  $PP_{13}PF_6$ .

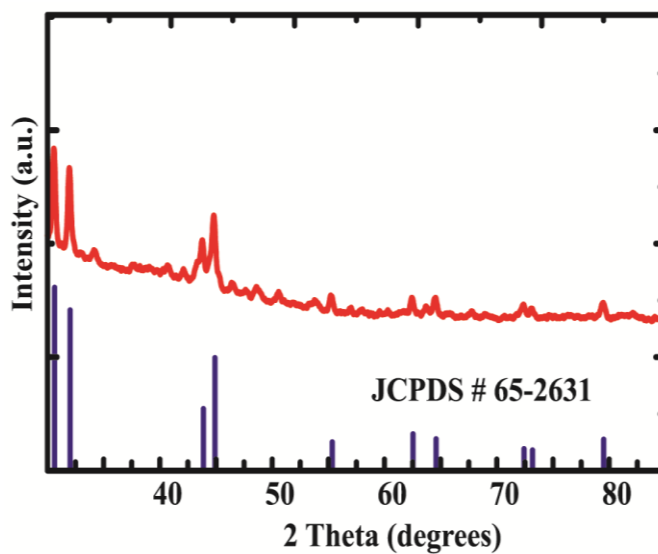


**Figure S2.** XRD of electrodeposited Sn over stainless steel electrode (red line) and blue lines shows the standard Sn (JCPDS#65-2631).

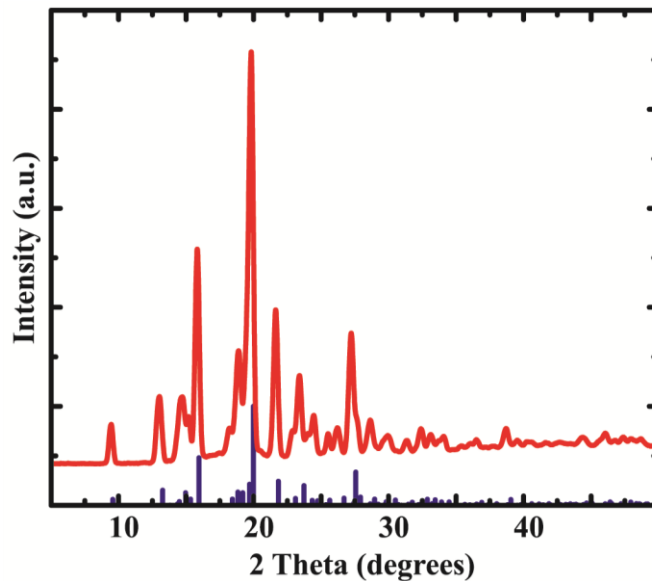


**Figure S3.** Experimental powder XRD of  $\text{PP}_{13}\text{PF}_6$  (red line) compared with the theoretically generated XRD pattern (blue line) using the single crystal structure.

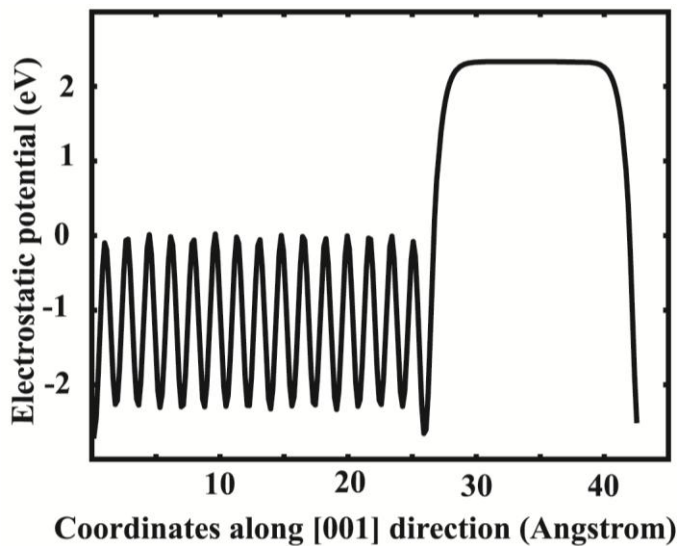


**Figure S4.** Calculated electrostatic potential of Li showing the lithium vacuum level at 2.33 eV. The Fermi-level is calculated as -0.67 eV.

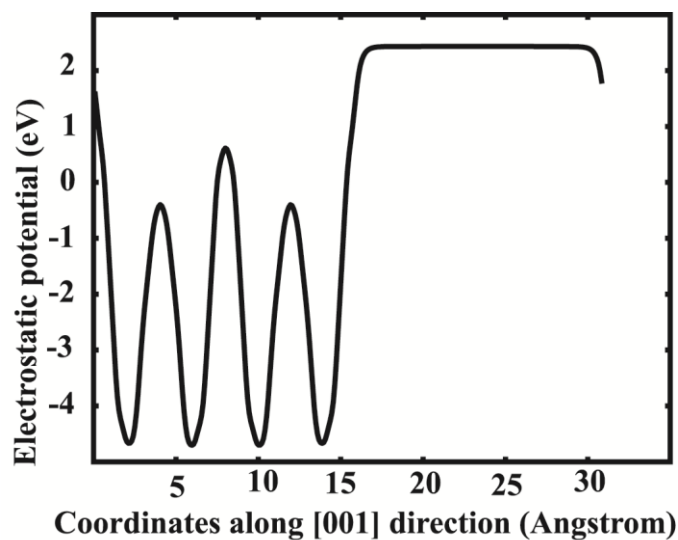


**Figure S5.** Calculated electrostatic potential of  $\text{PP}_{13}\text{PF}_6$ , showing a vacuum level of 2.39 eV and a Fermi-level of -6.20 eV.

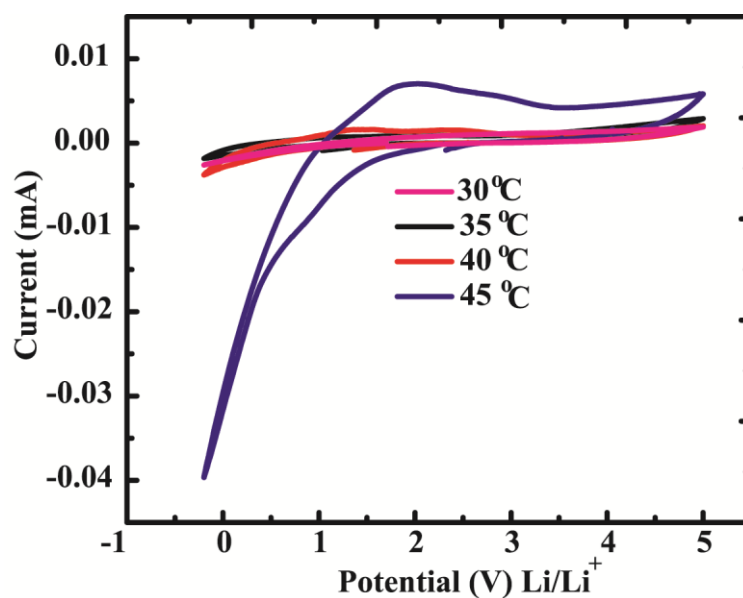


**Figure S6.** Cyclic voltammograms of  $\text{PP}_{13}\text{PF}_6$  using the asymmetric cell (Li metal/  $\text{PP}_{13}\text{PF}_6$  + 10wt% LiTFSI)/stainless steel block) with different temperatures at the scan rate of 2 mV/s.

**Table S1.** Impedance and conductivity data of symmetric and asymmetric cells.

| <b>Symmetric cell</b>  |                 |              |                      |                         |                |               |
|------------------------|-----------------|--------------|----------------------|-------------------------|----------------|---------------|
| <b>Temp (°C)</b>       | <b>Temp (K)</b> | <b>(1/K)</b> | <b>R<sub>p</sub></b> | <b>Conductivity (σ)</b> | <b>log (σ)</b> | <b>ln (σ)</b> |
| 22.7                   | 295.7           | 0.00338      | 76718                | 2.06E-06                | -5.6852        | -13.091       |
| 32                     | 305             | 0.00328      | 33994                | 4.66E-06                | -5.3317        | -12.277       |
| 35                     | 308             | 0.00325      | 24387                | 6.49E-06                | -5.18746       | -11.945       |
| 40                     | 313             | 0.00320      | 5059                 | 3.13E-05                | -4.50436       | -10.372       |
| 45                     | 318             | 0.00315      | 2158                 | 7.34E-05                | -4.13435       | -9.520        |
| <b>Asymmetric cell</b> |                 |              |                      |                         |                |               |
| 25                     | 298             | 0.00335      | 1.08E+05             | 3.78E-07                | -6.42296       | -14.789       |
| 30                     | 303             | 0.00330      | 1.66E+04             | 9.31E-06                | -5.03105       | -11.584       |
| 35                     | 308             | 0.00325      | 9.64E+03             | 1.61E-05                | -4.79401       | -11.039       |
| 40                     | 313             | 0.00320      | 2.24E+03             | 6.90E-05                | -4.16118       | -9.581        |
| 45                     | 318             | 0.00314      | 6.48E+02             | 2.39E-04                | -3.62166       | -8.339        |